PNAS RESEARCH ARTICLE | IMMUNOLOGY AND INFLAMMATION OPEN ACCESS

Splice factor polypyrimidine tract-binding protein 1 (Ptbp1) primes endothelial inflammation in atherogenic disturbed flow conditions

Jessica A. Hensel[a], Sarah-Anne E. Nicholas[a], Amy L. Kimble[a], Arjun S. Nagpal[a], Omar M. F. Omar[a], Jordan D. Tyburski[a], Evan R. Jellison[b], Antoine Ménoret[b], Manabu Ozawa[c], Annabelle Rodriguez-Oquendo[a], Anthony T. Vella[b], and Patrick A. Murphy[a,1]

Edited by Kristen Lynch, Raymond and Ruth Perelman School of Medicine at the University of Pennsylvania, Philadelphia, PA; received December 9, 2021; accepted June 14, 2022 by Editorial Board Member Alberto R. Kornblihtt

NF-κB–mediated endothelial activation drives leukocyte recruitment and atherosclerosis, in part through adhesion molecules Icam1 and Vcam1. The endothelium is primed for cytokine activation of NF-κB by exposure to low and disturbed blood flow (LDF)but the molecular underpinnings are not fully understood. In an experimental in vivo model of LDF, platelets were required for the increased expression of several RNA-binding splice factors, including polypyrimidine tract binding protein (Ptbp1). This was coordinated with changes in RNA splicing in the NF-κB pathway in primed cells, leading us to examine splice factors as mediators of priming. Using Icam1 and Vcam1 induction by tumor necrosis factor (TNF)-α stimulation as a readout, we performed a CRISPR Cas9 knockout screen and identified a requirement for Ptbp1 in priming. Deletion of Ptbp1 had no effect on cell growth or response to apoptotic stimuli, but reversed LDF splicing patterns and inhibited NF-κB nuclear translocation and transcriptional activation of downstream targets, including Icam1 and Vcam1. In human coronary arteries, elevated PTBP1 correlates with expression of TNF pathway genes and plaque. In vivo, endothelial-specific deletion of Ptbp1 reduced Icam1 expression and myeloid cell infiltration at regions of LDF in atherosclerotic mice, limiting atherosclerosis. This may be mediated, in part, by allowing inclusion of a conserved alternative exon in Ripk1 leading to a reduction in Ripk1 protein. Our data show that Ptbp1, which is induced in a subset of the endothelium by platelet recruitment at regions of LDF, is required for priming of the endothelium for subsequent NF-κB activation, myeloid cell recruitment and atherosclerosis.

endothelial | alternative splicing | inflammation | atherosclerosis | platelets

Significance

Plaque forms in low and disturbed flow regions of the vasculature, where platelets adhere and endothelial cells are "primed" to respond to cytokines (e.g., tumor necrosis factor-α) with elevated levels of cell adhesion molecules via the NF-κB signaling pathway. We show that the splice factor polypyrimidine tract binding protein (Ptbp1; purple) mediates priming. Ptbp1 is induced in endothelial cells by platelet recruitment, promoting priming and subsequent myeloid cell infiltration into plaque. Mechanistically, Ptbp1 regulates splicing of genes (e.g., Ripk1) involved in the NF-κB signaling pathway and is required for efficient nuclear translocation of NF-κB in endothelial cells. This provides new insight into the molecular mechanisms underlying an endothelial priming process that reinforces vascular inflammation.

Atherosclerosis is a disease characterized by chronic sterile inflammation, driven by leukocyte recruitment to arterial regions of low and disturbed flow (LDF). In these regions, endothelial expression of leukocyte adhesion molecules, such as Icam1, Vcam1, and P-, E-, and L-selectins, as well as cytokines, such as CCL2 (MCP1) and CCL5 (RANTES), mediate leukocyte recruitment (1, 2). Complete inhibition of these molecules, or of the NF-κB signaling pathway, suppresses leukocyte recruitment to the endothelium and reduces both acute and chronic inflammation in atherosclerotic plaque (3). The expression of these molecules is tightly regulated in endothelial cells (EC), primarily by NF-κB signaling. Activity of this pathway and expression of downstream leukocyte recruitment factors is low under quiescent conditions, but increased through both transcriptional and posttranscriptional mechanisms in response to circulating inflammatory cytokines. Not all areas of the vasculature are similarly affected however, as it is only regions exposed to LDF that exhibit elevated levels of adhesion molecules in response to NF-κB agonists (4).

Notably, LDF alone is insufficient to induce high levels of adhesion molecule expression; rather, it primes the ECs for subsequent activation by cytokines (4, 5). Several signaling pathways contribute to the acute priming of ECs, including shear sensing complexes and Klf2-mediated transcription (2, 6). In addition, under chronic disturbed flow conditions, ECs are exposed to changes in the subendothelial matrix (7–10) and to platelet and innate immune cell binding, each of which can further enhance inflammatory responses in the endothelium (11–13). Platelets are a particularly important contributor to atherogenesis, as their depletion nearly ablates plaque growth (14–17). Thus, it is important to understand how EC exposure to platelets under LDF conditions may drive a chronically primed state, hyperresponsive to circulating proinflammatory cytokines, and therefore atheroprone.

Alternative splicing, which is coordinated by the spliceosome but directed by hundreds of RNA-binding splice factor proteins in the cell, allows a single gene and

Author contributions: J.A.H., S.-A.E.N., and P.A.M. designed research; J.A.H., S.-A.E.N., A.L.K., A.S.N., O.M.F.O., J.T., E.R.J., A.M., and P.A.M. performed research; O.M.F.O., M.O., A.R.-O., and A.T.V. contributed new reagents/analytic tools; J.A.H., S.-A.E.N., O.M.F.O., and P.A.M. analyzed data; and J.A.H., S.-A.E.N., A.R.-O., A.T.V., and P.A.M. wrote the paper.

Competing interest statement: A.R.-O. is an owner of Lipid Genomics, Inc., Farmington, CT.

This article is a PNAS Direct Submission. K.L. is a guest editor invited by the Editorial Board.

[1]To whom correspondence may be addressed. Email: pamurphy@uchc.edu.

This article contains supporting information online at http://www.pnas.org/lookup/suppl/doi:10.1073/pnas.2122227119/-/DCSupplemental.

Published July 18, 2022.

pre-mRNA to encode multiple unique mRNA molecules and protein products. Alterations in the levels and activities of RNA-binding splice factors can allow a cell to rapidly modify the composition of signaling pathways. For example, increased inclusion of alternative exons EIIIA and EIIIB in fibronectin is linked to alterations in extracellular matrix composition, integrin binding, and increased NF-κB signaling (7, 10). We observed a platelet-dependent induction of alternative splicing in the arterial endothelium under chronic LDF conditions (18). Among the alternatively spliced transcripts were multiple regulators of the NF-κB signaling pathway, including canonical pathway components, such as Iκbκγ (Nemo) and regulators, such as fibronectin (18). Thus, we hypothesize that alterations in RNA-binding protein activity and function in endothelium exposed to LDF is an important step in endothelial priming for subsequent immune activation, myeloid recruitment, and atherogenesis. Here, we perform a targeted CRISPR screen of RNA-splice factors implicated in EC activation, and identify polypyrimidine tract binding protein (Ptbp1, or hnRNP I) as a critical mediator of EC activation, responsible for alterations in splicing in approximately half of the genes in the canonical tumor necrosis factor (TNF)-α/NF-κB signaling pathway, and required for nuclear translocation of NF-κB, and plaque inflammation and expansion in vivo.

Results

A CRISPR-Knockout Screen of Splice Factors Reveals a Requirement for Ptbp1 in EC Priming. In earlier work, we identified broad changes in RNA splicing patterns induced by exposure of arterial ECs to LDF, and found that the majority of these splicing changes depended on platelets (18). Nearly 80% of ∼7,000 alternative splicing changes observed are reverted by platelet depletion (*SI Appendix*, Fig. S1). Thus, we focused on splicing changes induced in the endothelium upon platelet recruitment, and aimed to identify upstream regulators of this splicing response that could be critical in coordinating EC priming. First, we took a bioinformatic approach, and assembled a list of candidate regulatory factors, based on 1) differential splice factor expression, 2) enrichment of motifs nearby regulated core exons, and 3) splicing of the factor itself, which is often an indication of splice factor activity and autoregulation (19). From this, we deemed 57 splice factors likely to be important in the regulation of splicing changes in ECs under these conditions (Fig. 1*A* and *SI Appendix*, Fig. S2).

To assess contributions of these splice factors to EC priming, we established an in vitro CRISPR-knockout (KO) pooled screening approach, which took advantage of our previous discovery that splicing patterns in cultured aortic ECs resemble ECs primed by LDF in vivo (18). Briefly, in this screen, five guides to each candidate splice factor were designed using established criteria, and cloned in a pooled fashion into a lentiviral construct containing Cas9 and the guide RNA (gRNA) expression site (*SI Appendix*, Fig. S3, with distribution of the representation in the library shown in *SI Appendix*, Fig. S3 *B* and *C*). Infection of a pool of TetOn-Sv40 immortalized aortic ECs at low multiplicity of infection (MOI < 0.3) yields a cellular pool in which most of the cells are predicted to be infected with a single viral particle (22% single infection, 3.7% more than single infection). Puromycin selection removes uninfected cells, and infected cells can then be separated by their behavior and effects of CRISPR-mediated gene excision. As screening coverage must be high enough so that each guide-mediated deletion is represented by hundreds or thousands of individual deletions, we performed our screens with a predicted ∼7,000 infected cells per guide (*SI Appendix*, Fig. S4).

Having established a cellular pool with targeting of each of our 57 candidate splice factors targeted in individual ECs, we could then screen for their activity in regulating EC activation. To determine the impact of splice factor deletion on EC activation, we treated aortic EC with TNF-α, and used induction of Icam1 and Vcam1 surface protein expression as measured by flow cytometry as the main readout for EC activation. gRNA targeting genes important in promoting priming should be found more often in cells with low Icam1 and Vcam1 responses than high responses, indicating that deletion of the targeted splice factors suppressed the TNF-α response (illustrated in *SI Appendix*, Fig. S3 *A6* and *A7*). Indeed, we could identify cells in our CRISPR pool that did not respond strongly to TNF-α (Fig. 1*B*, portion of red TNF-treated cluster, close to untreated blue cells, labeled "Low"). Importantly, we observed that this "low responder" phenotype was retained if we sorted these ECs, plated them, and then restimulated them, indicating their stable alteration by CRISPR editing (*SI Appendix*, Fig. S5). Using this approach and subsequent identification of enriched gRNA in low and high responders by: 1) PCR amplification of lentiviral insertions, 2) high-throughput sequencing, and 3) statistical analysis, we found that Ptbp1 gRNA was consistently enriched in EC with a reduced Icam1 and Vcam1 surface protein response to TNF-α across multiple screens (Fig. 1*C* and Dataset S1), and through iterative screens (low response cells plated and treated again with TNF-α to determine those that retained a low response to TNF-α) (Dataset S1).

To determine whether impaired Icam1 and Vcam1 induction in ECs containing Ptbp1 gRNA might be a result of generally impaired cell function, we examined the presence of Ptbp1 gRNA at early and late timepoints in our pool of cells. Losses could represent reduced cell viability or proliferation, while gains could reveal growth-suppressive splice factors, as deletion of these genes would allow these cells to expand within the pool over time. We found no significant loss or enrichment of Ptbp1-targeting gRNA, while we did observe reduced representation of other gRNA and increased representation of gRNA for Hnrnpa1, a splice factor that has been shown to inhibit cell proliferation in other contexts (Fig. 1*D* and Dataset S2) (20).

If Ptbp1 promotes splicing responses and inflammation in LDF conditions, we would predict that Ptbp1 expression may be increased, and that its motifs would be enriched nearby splicing events regulated by platelet recruitment under LDF. Analysis of RNA transcripts from low flow arterial EC showed an increase in Ptbp1 RNA expression (Fig. 2*A* and *SI Appendix*, Fig. S6), and that this induction was dependent on platelets (Fig. 2 *A*, compare Δplatelets with ΔFlow to control with ΔFlow). Motif analysis indicated an enrichment of Ptbp1 motifs nearby exons alternatively spliced in an LDF- and platelet-dependent manner, consistent with increased activity of the splice factor (Fig. 2*C*). As recent work has highlighted the differential responses of ECs within atheroprone vessels (21–24), and even in the same LDF environment (22), we therefore examined single-cell data from carotid arteries exposed or not to LDF. We clustered EC populations from 2 d or 2 wk after surgical induction of disturbed flow as compared to normal flow EC cells from the contralateral artery (Fig. 2*D*), and then identified key cell types based on marker gene expression (Fig. 2*E*). Ptbp1 was prominently expressed in two low-flow EC clusters, EC5 ($n = 386$ cells, 28% of 2 d ECs and 4% of 2 wk disturbed flow ECs) and EC7 ($n = 197$ cells, 7% of 2 d ECs and 8% of 2 wk disturbed flow

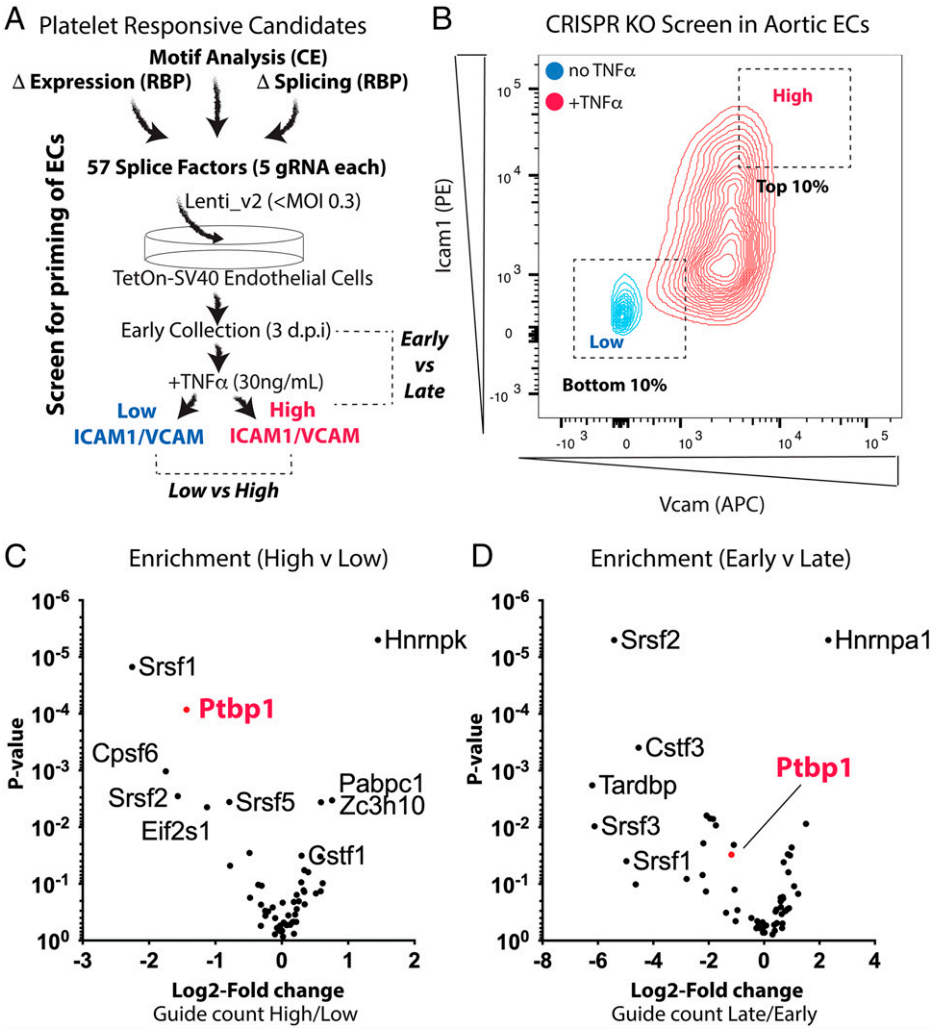

Fig. 1. CRISPR-KO screen to examine splice factor involvement in endothelial priming. (*A*) In vitro screen to identify RNA binding proteins required for endothelial priming. d.p.i., days postinfection with CRISPR library. (*B*) Example overlaid flow cytometry plots, showing Icam1 and Vcam1 protein expression in the CRISPR KO pool of aortic ECs before (blue) and after (red) treatment with TNF-α. Dashed boxes represent the regions of the TNF-α–treated cluster analyzed for guides resulting in low or high responses. (*C* and *D*) MAGeCK analysis of differentially detected gRNA in cells from *C* in cells with a high Icam1 and Vcam1 response versus cells with a low response or (*D*) early passage after lentivirus infection (3 d postinfection) or late passage after infection (2 wk postinfection). Data in *C* and *D* are grouped by gene (5 gRNA per gene). Enrichment in guide count (*x* axis) and *P* value (*y* axis) are shown. CE, core exon; RBP, RNA-binding protein. Statistical analysis was performed as follows: (*C* and *D*) MAGeCk was used to obtain $\log_2$ fold-change and *P* value, using a negative binomial model.

ECs) (Fig. 2 *F* and *G*). Notably, these clusters (EC5 and EC7) were associated with higher levels of adhesion molecules Icam1, Vcam1, P- and E-selectin (Fig. 2*H* and Dataset S3). Both clusters exhibited a signature of Myc signaling (50 of 200 top genes in EC5 and 21 of 200 in EC7, false-discovery rate [FDR] = 5E-19), but EC7 was primarily associated with TNF signaling (27 of 200 genes, FDR = 8E-28). Therefore, Ptbp1 expression is induced in a platelet-dependent manner, under low-flow conditions, and is maintained in a subset of the EC under chronic LDF conditions, where increased expression of key NF-κB–responsive leukocyte recruitment genes is evident.

Endothelial Ptbp1 Is Required for NF-κB–Mediated Transcriptional Activation. We next focused on the mechanism through which Ptbp1 might lead to increased Icam and Vcam1 expression. As the NF-κB signaling pathway is critical for induction of these transcripts, we examined NF-κB transcriptional activation by using a modified a lentiviral NF-κB reporter (25) to introduce eGFP as the reporter gene downstream of the NF-κB binding motif (Fig. 3*A*). Using this reporter, we again screened splice factors in a CRISPR-KO pool of aortic ECs. Ptbp1 gRNA was enriched in ECs with reduced NF-κB activity in response to TNF-α stimulation as measured by decreased GFP fluorescence (Fig. 3*B*), showing that deletion of Ptbp1 impairs TNF-α–mediated NF-κB transcriptional responses.

To validate these results and confirm specificity, we generated independent CRISPR-KO aortic EC clones, using two different Ptbp1 gRNA, as well as a set of nontargeting gRNA single-cell clones (Fig. 3*C*). Furthermore, we rescued Ptbp1 expression in these Ptbp1 KO clonal lines with a human PTBP1 cDNA construct (Fig. 3*C*) validating loss and restoration by Western blot (Fig. 3*D*) and immunofluorescence (Fig. 3*E*). We then examined the NF-κB response to TNF-α, and found that this was blocked by the loss of Ptbp1, and restored with the PTBP1 rescue (Fig. 3*F*, with quantification in Fig. 3*G*). Multiple single-cell clones from different gRNA exhibited the same response, further verifying these results (Fig. 3*H*). Notably, as we had previously observed in our screens, loss of Ptbp1 had little effect on EC survival or proliferation, as we found no significant differences in proliferation, or in their levels of cell death (by propidium iodide uptake), among these EC lines (*SI Appendix*, Fig. S7).

The NF-κB signaling pathway is a common downstream mediator of many upstream inputs—including TNF-α, Il1β, and LPS—each of which signal through different receptors at the plasma membrane. To understand whether Ptbp1-mediated NF-κB inhibition was specific to TNF-α, or whether it may act on the core pathway downstream of these multiple inputs, eGFP expression was examined at multiple timepoints in CRISPR-KO cells along with WT and gRNA control cells were examined. We found a similar inhibition of eGFP induction downstream of Il1β and LPS stimulation in Ptbp1 CRISPR-KO cells, beginning as early as 6 h (Fig. 3 *I*–*K*), suggesting that loss of Ptbp1 inhibits core NF-κB signaling.

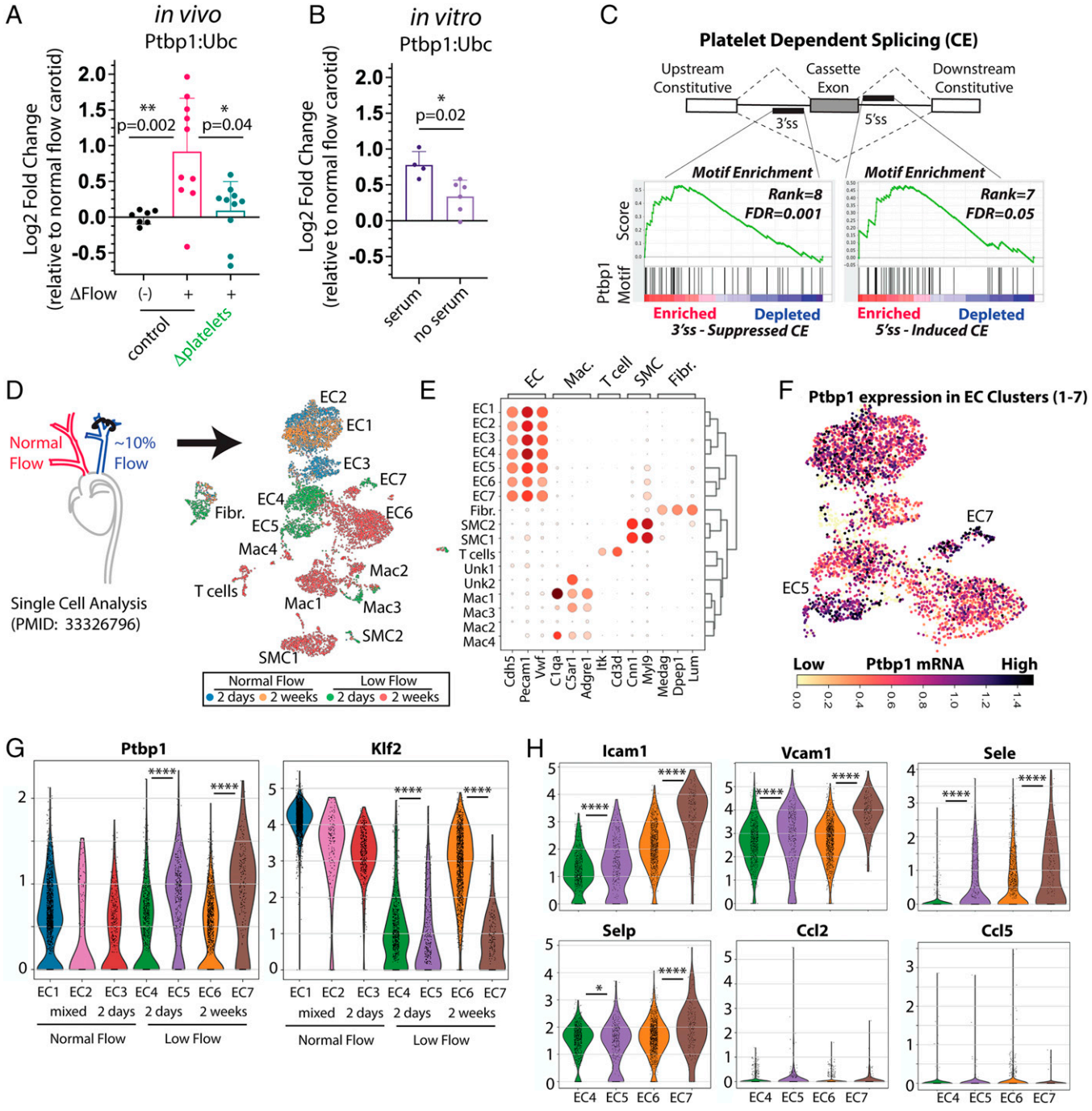

Fig. 2. Platelet-dependent induction of Ptbp1 in inflammatory ECs under low-flow conditions. (*A*) Expression of Ptbp1 mRNA in intimal flush from carotids exposed to LDF (ΔFlow) by partial carotid ligation or not (contralateral) by partial carotid ligation, or exposed to disturbed flow with platelet depletion (Δplatelets), as measured by qPCR against housekeeping gene Ubc. Each point represents data from one artery. (*B*) Expression of Ptbp1 mRNA in isolated aortic ECs cultured in the presence or absence of serum, by qPCR. Each point represents data from a biological replicate well. (*C*) Kolmogorov–Smirnov based enrichment of in vitro defined Ptbp1 6-mer motifs nearby regulated core exons, relative to skipped exons which were not altered by the loss of platelets under LDF conditions. Rank displayed is relative to all other splice factor motifs searched. (*D*) Approach and Leiden clustering of publicly available single cells data from intimal digest, isolated from low flow or normal flow artery at 2 d and 2 wk after ligation. (*E*) Heat map plot showing defined cell clusters from the intima and marker genes. (*F*) Expression of Ptbp1 in EC clusters in the data. (*G*) Violin plots showing expression of Ptbp1 and Klf2 in each EC cluster. Bar below the graph indicates source of the ECs in the cluster. Each cell in the plot is indicated by a point. (*H*) Similar violin plots of key inflammatory response genes in low flow EC clusters. Statistical analysis was performed as follows: (*A*) Kruskal–Wallis and Dunn's post hoc analysis, (*B*) Mann–Whitney test, (*C*) Kolmogorov—Smirnov analysis integrated into the GSEA work flow, and (*G* and *H*) Wilcoxon rank test, comparing gene expression levels in EC4 to EC5 and EC6 to EC7, $*P < 0.05$, $**P < 0.01$, $****P < 0.0001$.

As our work focused on a single synthetic NF-κB–responsive element, we tested if endogenous NF-κB–mediated transcription was similarly affected. We performed RNA-sequencing analysis on WT ECs, the Ptbp1 CRISPR-KO EC line, and human PTBP1 rescue of these Ptbp1 CRISPR-KO ECs, before and after treatment with TNF-α. As expected, TNF-α stimulation led to large changes in transcription of canonical NF-κB target genes. Analysis of the top 200 induced transcripts found in WT cells showed little or no response to TNF-α in the Ptbp1 CRISPR-KO cells, and that this could be rescued by human PTBP1 cDNA (Fig. 3*L* and Dataset S4). Analysis of individual transcripts in this response shows a strong effect on

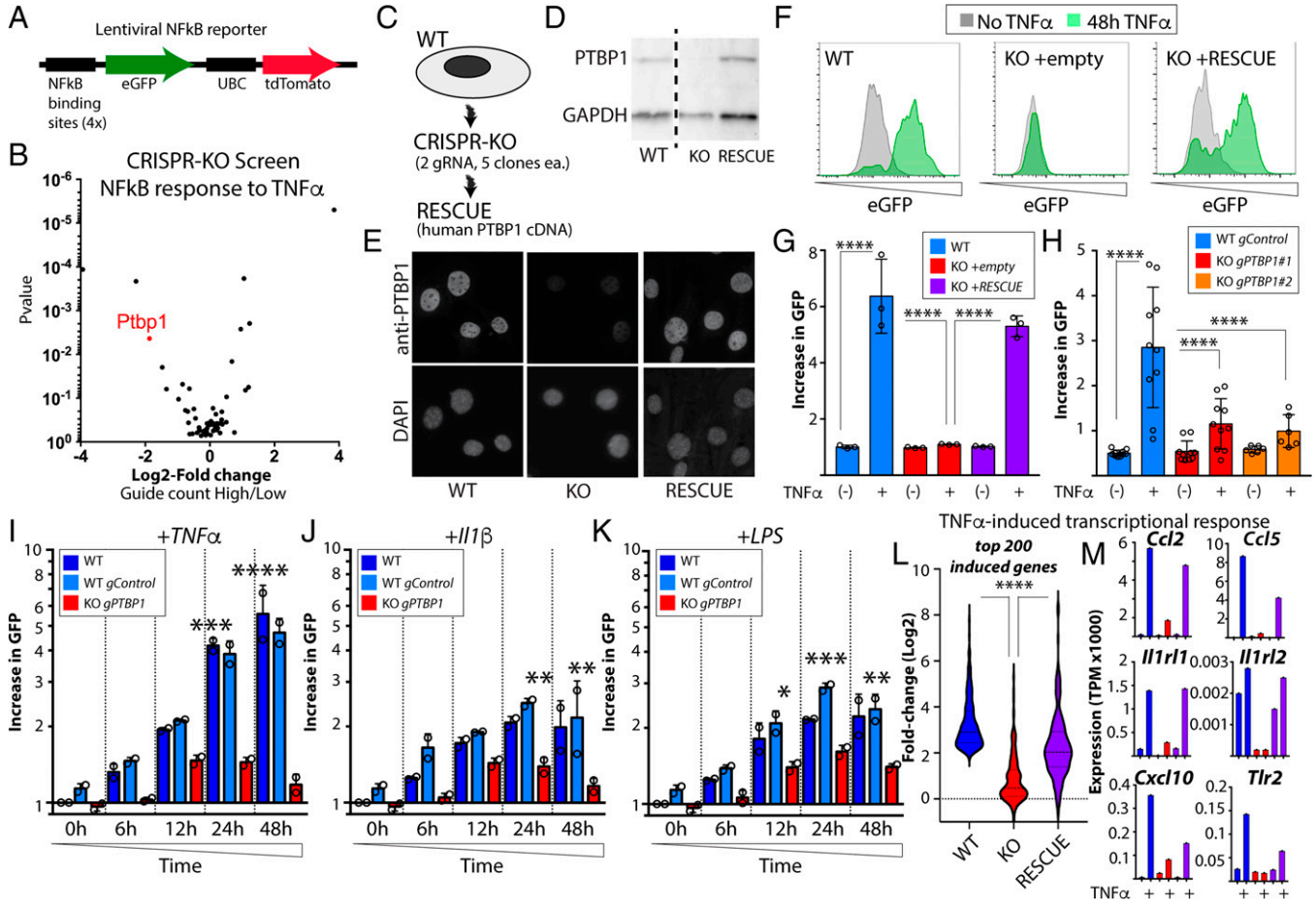

Fig. 3. Endothelial Ptbp1 is required for NF-κB–mediated transcriptional responses. (*A*) Engineered lentiviral NF-κB reporter, used to assess NF-κB transcriptional activity. UBC, ubiquitin C promoter, used to drive constitutive tdTomato expression, a control for Lentiviral expression in the cells. (*B*) MAGeCK analysis of results of CRISPR KO pool, using NF-κB reporter to examine response to TNF-α. (*C*) Schematic showing approach to determine the effect of endothelial Ptbp1 on endothelial "priming." (*D*) Western blot and (*E*) immunostaining of cells (63x), showing antibody staining of PTBP1 and GAPDH in a representative CRISPR-KO single-cell clone and this clone with reexpression of human PTBP1 cDNA. (*F*) Single-cell clone of Ptbp1 CRISPR KO, showing NF-κB response by reporter, and restoration of TNF-α response by human PTBP1 cDNA rescue construct. (*G* and *H*) Quantitation of mean increase in eGFP expression in each cell line after TNF-α treatment. (*G*) Each replicate is a biological replicate in the in vitro assay. (*H*) Replicates include multiple single-cell clones for each control guide (gControl) or Ptbp1 targeting guides (gPTBP1). (*I*–*K*) Quantitation of mean increase in eGFP over time for cells with NF-κB reporter only, cells with reporter + control guide (gControl), or Ptbp1 targeting guide (gPTBP1). Stimulation at 0 h with (*I*) 30 ng/mL TNF-α, (*J*) 30 ng/mL Il1β, or (*K*) 30 ng/mL LPS. (*L*) Analysis of the top 200 TNF-α–induced transcripts in WT cells, Ptbp1 KO cells, and rescue cells, as determined by RNA-sequencing analysis of the cell lines before and after 24 h of 30 ng/mL TNF-α. (*M*) Examples of transcripts from *L*, showing expression levels. Statistical analysis was performed as follows: (*G*, *H*, and *L*) Kruskal–Wallis with Dunn's multiple comparison test, (*I*–*K*) two-way ANOVA with post hoc Tukey's multiple comparisons test; ****$P < 0.0001$, ***$P < 0.001$, **$P < 0.01$, *$P < 0.05$.

the TNF-α–meditated induction of several genes critical in endothelial inflammatory responses, including Vcam1, Icam1, P- and E-selectin, Ccl2, Ccl5, Il1rl1, Il1rl2, Cxcl10, and Tlr2 (Fig. 3*M* and Dataset S4).

Thus, Ptbp1 is critical for NF-κB signaling responses in ECs, downstream of various inputs. Expression of Ptbp1 primes EC to respond to TNF-α, Il1β, and LPS, licensing them to express a wide range of genes involved in the recruitment of leukocytes.

Ptbp1 Is Required for Efficient Nuclear Translocation of NF-κB and Modulates Alternative Splicing of Core NF-κB Genes. As nuclear translocation of the RelA/p65 component of the NF-κB heterodimer is a critical step in NF-κB transcriptional activation, we examined this step following TNF-α stimulation of the aortic ECs. We found that deletion of Ptbp1 almost entirely blocked TNF-α–induced nuclear translocation of RelA/p65, as measured by immunofluorescence (Fig. 4 *A* and *B* and *SI Appendix*, Fig. S8) or Western blot of isolated nuclei (Fig. 4 *C* and *E*) in two separate CRISPR-KO clones. These responses were rescued by the expression of human PTBP1 cDNA in the same clones. Notably, changes in the level of Ptbp1 had little effect on cytoplasmic levels of RelA/p65, consistent with a specific effect on nuclear translocation (Fig. 4 *D* and *E*).

To determine how changes in Ptbp1 levels might affect the NF-κB signaling pathway, we examined changes in RNA splicing which were lost in Ptbp1 CRISPR-KO cells and restored with human PTBP1 cDNA. In total, we identified 180 splicing changes in the Kyoto Encyclopedia of Genes and Genomes NF-κB pathway genes, 93 with a splicing difference of >10%, and 48 with a splicing difference >20% (*SI Appendix*, Fig. S9 *A* and *B* and Dataset S5). In these datasets, splicing levels at a particular junction are indicated by the percent spliced in (Psi), where a Psi of 0.1 = 10% spliced and 0.9 = 90% spliced in. Additionally, cDNA rescue using human PTBP1 in the KO cell line is sufficient to restore the splicing pattern of these genes, demonstrating that these splicing patterns are strongly dependent on Ptbp1 levels (*SI Appendix*, Fig. S9*B*).

To determine whether Ptbp1 affected splicing of genes in the platelet-mediated EC activation we previously observed (*SI*

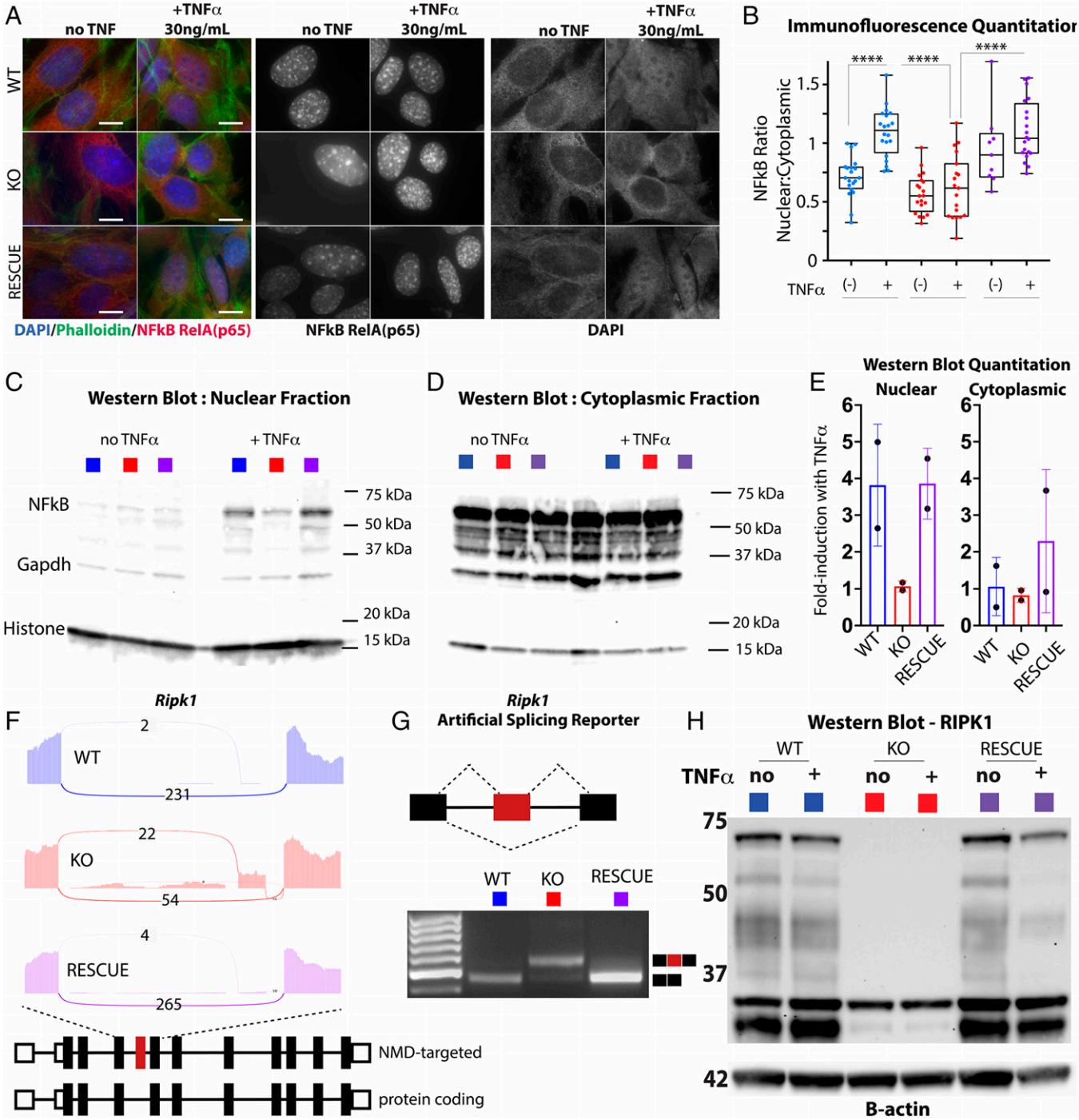

Fig. 4. Ptbp1 is required for the nuclear translocation of NF-κB and efficient expression of Ripk1. (*A*) Immunofluorescence staining of NF-κB in murine aortic EC with deletion of Ptbp1 (KO) or rescue with human Ptbp1 (RESCUE), before and after 24-h treatment with 30 ng/mL TNF-α. (Scale bars, 10 μm.) (*B*) Quantitation of nuclear translocation of NF-κB, presented as the ratio between nuclear and cytoplasmic staining. Each point represents a measured cell. (*C* and *D*) Western blot from the nuclear enriched (*C*) or cytoplasmic (*D*) fractions of aortic EC from the cell lines indicated in the key, with or without 24-h treatment with 30 ng/mL TNF-α. (*E*) Quantification of signal normalized to housekeeping protein (Histone in nuclear and Gapdh in cytoplasmic); fold-induction relative to cells before TNF-α stimulation. Replicates indicate separate experiments with separate CRISPR-KO clones and rescues in these clones. (*F*) Sashimi plot of the indicated region in Ripk1 transcript from RNA-sequencing, showing the number of reads spanning or including the Ptbp1-suppressed exon. (*G*) Plasmid minigene reporter of the Ripk1-suppressed exon, and PCR analysis of inclusion in the indicated cell lines after transfection. (*H*) Western blot showing probe for Ripk1 and reprobing for betaActin, with molecular weights on ladder indicated. (*B*) Kruskal–Wallis with Dunn's multiple comparison test, ****$P < 0.001$.

Appendix, Fig. S1), we examined the overlap between platelet regulated transcripts from that in vivo dataset and those identified here in vitro, limiting to splicing events with at least five supportive reads in both sets. We found evidence for Ptbp1 regulation of ∼25% of all the platelet-regulated splicing events (*SI Appendix*, Fig. S9*C*). Analysis of these splicing events revealed that those with reduced inclusion upon platelet depletion also showed reduced inclusion upon Ptbp1 depletion (*SI Appendix*, Fig. S9*D*), consistent with increased Ptbp1 activity in EC under LDF in the presence of platelets under LDF.

The pervasive effects on the NF-κB signaling pathway suggests many ways in which altered splicing might affect nuclear localization of NF-κB. To obtain a better understanding of these effects, we performed RNA and Western blot analysis of key NF-κB

components in these cells. We found similar levels of the TNF receptor, Ikba, and Ikkab, as well as the phosphorylation of these components regardless of Ptbp1 expression (*SI Appendix*, Figs. S10 and S11). However, we noticed a substantial reduction in Ripk1 mRNA levels as a result of Ptbp1 KO (*SI Appendix*, Fig. S11). As splicing of Ripk1 was found to be regulated by Ptbp1, we examined the splicing change in more detail. We found that the Ripk1 splicing event detected upon Ptbp1 KO resulted in the inclusion of a skipped exon not found in common annotations (Fig. 4*F* and *SI Appendix*, Fig. S12 *A–C*). Notably, however, this splicing change had also been previously reported as a Ptbp1-suppressed exon which, when included, targets the transcript for nonsense-mediated decay (NMD) in fibroblasts (26). This splice isoform, containing multiple adjacent high-confidence Ptbp1 binding sites, results in the inclusion of a premature stop codon (*SI Appendix*, Fig. S12*D*). A minigene reporter of this splicing event transfected into cells with and without Ptbp1 revealed a strong change in splicing regulation. In the presence of Ptbp1, the NMD-targeting exon is barely detectable, whereas loss of Ptbp1 results in the majority of transcript containing this exon (Fig. 4*G*). Additionally, the reduction in Ripk1 transcript led to a nearly complete loss in Ripk1 protein (Fig. 4*H*). Notably, while the level of this Ptbp1-regulated exon is normally low in EC, it is detected and regulated consistent with Ptbp1 regulation (e.g., lowest inclusion levels are in the low flow carotid artery without platelet depletion) (*SI Appendix*, Fig. S12*F*). Furthermore, inclusion levels of the exon are inversely correlated with Ripk1 expression in these ECs, suggesting that Ptbp1 regulation of Ripk1 via splicing may contribute to its expression in the artery wall. Consistent with this, Ripk1 is significantly elevated in the Ptbp1 cluster of ECs exhibiting enhanced TNF-α signaling (EC5).

While this single change in Ripk1 splicing and protein levels is likely to contribute to the reduced nuclear translocation of NF-κB, we cannot rule out impacts from the many other changes in core and regulatory components of the pathway. For example, we also observed an increase in inclusion of a protein-coding cassette exon in a disordered region of the Pdlim7 protein (*SI Appendix*, Fig. S9 *E–G*) that may also be relevant to reduced transcriptional output, as Pdlim7 promotes degradation of the p65 subunit of NF-κB (27). Future work will be required to assess the effects of the other Ptbp1-regulated splicing events on NF-κB signaling responses.

Ptbp1 Expression Positively Associates with Plaque Burden and TNF-α/NF-κB Signaling Pathway in Human Arteries. If Ptbp1 is required for efficient TNF-α/NF-κB signaling responses, then increased PTBP1 RNA expression might be correlated with these same signaling pathways in human tissues. To test this, we examined the GTEx database, which contains RNA transcript analysis and pathology reports from hundreds of donor arteries (Fig. 5*A* and *SI Appendix*, Fig. S13). While this database is focused on nondiseased tissues, nearly all arteries in the donor group collected include some degree of plaque formation, reflecting the ubiquitous nature of this process in human arteries with age. Nevertheless, a small subset of arteries was deemed free, or mostly free of plaque by pathology report (Fig. 5*B*), while others had increasing levels of plaque (Fig. 5*C*). As expected, expression of TNF-α and Il1β, cytokines central to plaque development and immune cell composition, were enriched in arteries with plaque versus those without (Fig. 5 *D* and *E*). PTBP1 and transcriptional markers of NF-kB activity, like the interleukin 1 receptor-like 1 (ILRL1) receptor, were also increased in arteries with plaque versus those without (Fig. 5 *F* and *G*). Notably, there is a wide range of expression of both cytokines and their receptors in plaque, reflecting widely varied immune milieus within plaque (Fig. 5 *D–G*). This variation is important, as immune cell composition in plaque is strongly correlated with myocardial infarction and stroke.

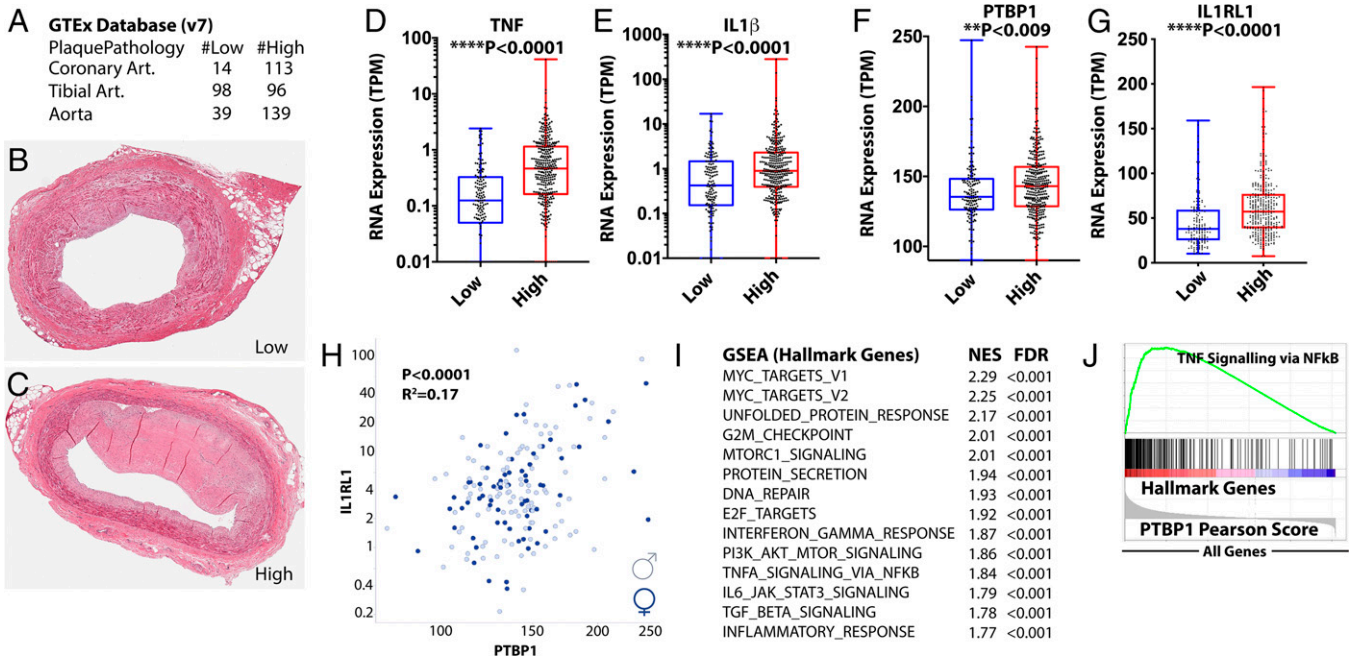

Fig. 5. PTBP1 expression correlates with plaque and expression of TNF pathway genes in human arteries. (*A*) Summary of arteries (Art.) of each type with indicated pathology data from the GTEx database (v7). (*B* and *C*) Examples of histological sections used for analysis of plaque characteristics in the GTEx database, showing examples of low (*B*) and high (*C*) plaque. (*D–G*) Analysis of expression of the indicated genes in arteries separated by low and high plaque phenotype. Each point in *D–H* represents a single artery sample. (*H*) Gene–gene correlation between the expression of PTBP1 and IL1RL1 in human coronary arteries, where sex is indicated by different shading (gray = female; male = black). (*I*) Top GSEA Hallmark Gene Groups associated with genes most associated with Ptbp1 (highest Pearson scores). NES, normalized enrichment score. (*J*) Example GSEA plot, showing the location of TNF signaling via NF-κB Hallmark Genes among those most associated with PTBP1 expression (left side of the Pearson score plot). (*D–G*) Mann–Whitney *U* test.

Therefore, we asked what pathways are most associated with PTBP1 in coronary arteries by examining gene–gene correlations with PTBP1 expression (e.g., IL1RL1) (Fig. 5*H* and Dataset S6). Doing this for all genes in specific arteries (e.g., coronary, tibial, aorta) revealed a strong conservation of gene–gene interactions between arteries (*SI Appendix*, Fig. S13), but those genes that correlated with PTBP1 in arteries did not have the same correlation in whole blood (*SI Appendix*, Fig. S13), indicating a set of artery specific correlations. Notably, among the genes correlated with PTBP1 in arteries were several regulated by PTBP1 in our Ptbp1 CRISPR-KO cells (e.g., CCL2, Pearson 0.49, IL1RL1 Pearson = 0.41, RIPK1 Pearson = 0.33, VCAM1 Pearson = 0.2, ICAM1 Pearson = 0.31, SELP Pearson 0.24) (Dataset S6). We then asked what gene groups are most often positively correlated with PTBP1 expression in arteries, and found a strong signature for Myc (which can induce Ptbp1 expression, and is also regulated by PTBP1) (28–30), but also interferon (INF)-γ signaling, and TNF-α signaling via NF-κB (Fig. 5 *K* and *L* and Dataset S6).

Thus, in human arteries, PTBP1 expression in plaque correlates with RNA markers of TNF-α pathway activity and the expression of many of these same genes were found in Ptbp1-regulated in murine aortic ECs (e.g., IL1RL1, ICAM, and VCAM1). While these findings in human arteries are correlative so far, we note that a SNP in Ptbp1 is associated with increased levels of C-reactive protein levels (rs123698-G, P = 1e-9) (31), a marker of systemic inflammation and cardiovascular disease risk (32).

Endothelial-Specific Ptbp1 Deletion Limits Endothelial Activation and Immune Recruitment to Plaque in Mice. Our data showing a required role for Ptbp1 in EC priming, and the observation that human PTBP1 RNA levels are increased in arteries with plaque and TNF-α pathway activation suggested a possible requirement for Ptbp1 in plaque inflammation and atheroma growth. To test this in vivo, and in the context of atherosclerosis, we generated a conditional endothelial specific Ptbp1 mouse [*Cdh5(PAC)CreERT2; Ptbp1*^{ff} or EC-KO], by intercrossing mice with these alleles (33, 34). We induced Ptbp1 excision in 6- to 7-wk-old mice by tamoxifen treatment. ECs isolated from these mice confirmed the loss of Ptbp1, as well as the Ripk1 splicing and expression pattern we had observed in the CRISPR-KO and human PTBP1 rescue cells (*SI Appendix*, Fig. S14 and S15). *En face* imaging of arterial vessels confirmed the loss of Ptbp1 protein (*SI Appendix*, Fig. S16).

We then induced hypercholesteremia by treating Ptbp1 EC-KO mice or their littermate controls with gain-of-function mAAV-PCSK9^{D377Y} and a high-fat diet (HFD) (35). We collected mice in two cohorts, focusing on the early stages of plaque development (3 mo, when plaque is not yet apparent in descending aorta, but has appeared in the innominate artery and aortic arch) and late stages (5 and 7 mo, when plaque extends through the length of the descending aorta). WT mice exhibited robust plaque in both the innominate artery at 3 mo and the descending aorta at 5 to 7 mo (Fig. 6 *A*–*E*). At both collections, analysis of serum revealed that total cholesterol levels were elevated ∼10-fold over baseline levels in adeno-associated virus (AAV)/HFD-treated mice, regardless of genotype (Fig. 6*F*). Despite similar cholesterol levels in Ptbp1 EC-KO mice, they exhibited significantly lessened plaque development in both the innominate artery (3-mo-old mice), and the descending aorta (5- and 7-mo-old mice), demonstrating a requirement for endothelial Ptbp1 in plaque development. Importantly, platelets were not altered in these mice; rather, we altered the downstream EC response to platelets via Ptbp1.

To examine the status of EC activation within plaque, we performed immunofluorescence staining of the innominate arteries. Consistent with our in vitro data, expression of Icam1 was impaired in the CD31^{+} lining of EC-KO arteries with plaque relative to littermate controls (arrowheads in Fig. 6 *G* and *H*). Although littermate controls to the EC-KO mice exhibited a large range in plaque severity, even the least severe of these showed increased Icam1 expression relative to unaffected distal regions of the carotid from these mice or Ptbp1 EC-KO mice.

To determine whether the Ptbp1 regulation of EC activation affected the abundance of myeloid cells in the plaque, we stained innominate plaque for macrophages (Mac3) and quantified area coverage. We found a trend toward reduced staining in Ptbp1 EC-KO mice (Fig. 6 *I* and *J*). While the innominate artery is an excellent model for mature plaque development, its small size limits a quantitative analysis of immune cells by flow cytometry. Therefore, we performed quantitative analysis of myeloid cell numbers by flow cytometry (CD45^{+}CD11b^{+}CD3^{-}) in the aortic arch, another disturbed flow region of plaque formation. To focus on plaque immune cells, we removed the adventitia prior to digestion and cell isolation. We found a significant reduction in plaque immune cells at both early (Fig. 6 *K*–*M*) and late time points (*SI Appendix*, Fig. S17).

Therefore, Ptbp1 deletion from the endothelium reduces Icam1 expression in regions of vascular priming and impairs myeloid cell accumulation, consistent with the reduced levels of priming we observed in cultured cells.

Discussion

Here, through a focused CRISPR-KO screen of splice factors involved in the early endothelial response to LDF, we found that Ptbp1 is required for endothelial priming. Ptbp1 expression and downstream splicing responses are induced and sustained in a proinflammatory subset of arterial ECs in an LDF environment in a platelet-dependent manner. They express high levels of NF-κB transcriptional targets Icam1, Vcam1, and E- and P-selectin and cytokines Ccl2 and Ccl5. Deletion of Ptbp1 from arterial ECs affects alternative splicing in the canonical TNF/NF-κB signaling pathway, most notably including an NMD targeted alternative splicing event in Ripk1, and results in the suppressed nuclear translocation of the RelA/p65 subunit of NF-κB and transcriptional activity. As PTBP1 RNA expression in human coronary arteries correlates with plaque and expression of NF-κB transcriptional targets, and in vivo endothelial-specific deletion of Ptbp1 reduces adhesion protein expression, myeloid cell recruitment, and plaque development in regions of LDF, we propose that platelet recruitment to the endothelium in regions of LDF primes the endothelium for enhanced inflammatory responses by increasing the levels of Ptbp1, resulting in changes in RNA splicing patterns in the NF-κB signaling pathway and increasing NF-κB nuclear localization and transcription of downstream genes.

Contextual Role of Ptbp1 in Priming Acute and Chronic Inflammatory Responses. In this work, we have used a simplified in vitro model to understand the role of RNA-binding protein expression on EC priming, and to show that this process depends on platelet recruitment. We have previously shown that ECs cultured in vitro under serum and static conditions exhibit an expression and splicing profile that mimics activated carotid endothelium in vivo, after exposure to partial carotid

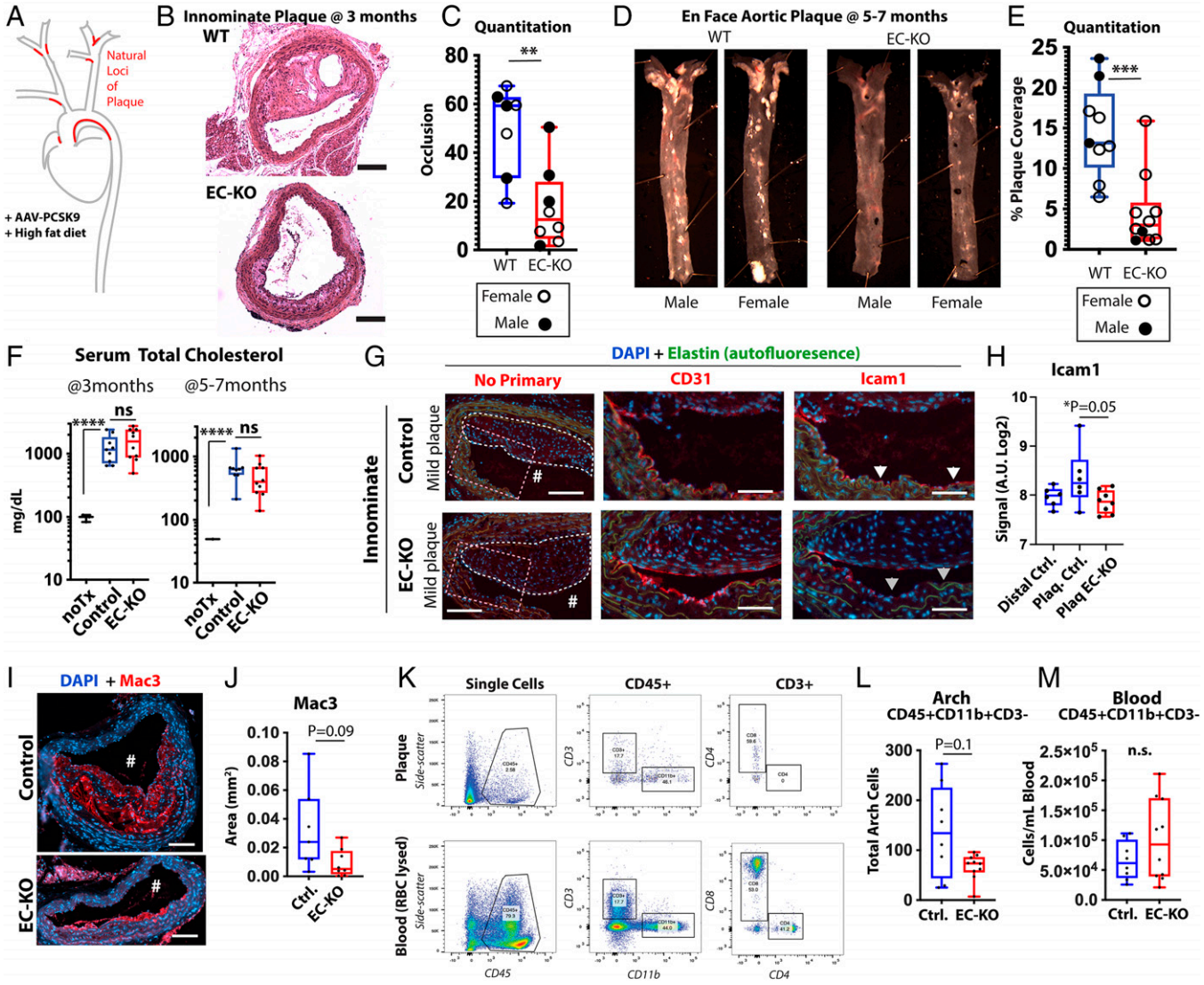

Fig. 6. Hypercholesteremic Ptbp1 EC-KO mice exhibit reduced plaque and impaired recruitment of myeloid cells to the aortic arch. (*A*) Schematic of model, showing treatment protocol with AAV-PCSK9 + HFD and LDF sites of plaque deposition (red). (*B*) Representative H&E images of innominate artery branch point images at 3 mo and (*C*) quantitation of plaque occlusion of indicated genotypes. (Scale bars, 100 μm.) (*D*) Representative images of aorta from the indicated genotypes taken at 5 mo after AAV-PCSK9 + HFD, with quantitation (*E*). (*F*) Plasma cholesterol levels in untreated mice (noTx) and the Ptbp1 EC-KO mice and their littermate controls (EC-KO and Control), 3 mo or 5 to 7 mo after treatment with AAV-PCSK9 and HFD. (*G*) Immunofluorescent images of innominate artery plaque in EC-KO mice and littermate controls. Lumen is indicated with a hashtag (#) and neointimal plaque with the white dotted line. Areas from the boxed region is shown at higher magnification with the antibodies indicated. (Scale bars, 100 μm; *Inset*, 50 μm.) (*H*) Quantification of image pixel intensity in the lining of these vessels. In the graph, each point represents the innominate artery from a different mouse. Control mice were measured at the location of the branch point and plaque (Plaq. Ctrl.) and more distally (Distal Ctrl). EC-KO mice were measured only at the site of the branch point and plaque. (*I*) Immunofluorescent images of innominate artery plaque in EC-KO mice and littermate controls, stained for Mac3. (Scale bars, 100 μm.) (*J*) Quantitation of the $Mac3^+$ thresholded area of plaque from each mouse examined. (*K*) Representative flow cytometry data from aortic arch and blood, showing gating of $CD45^+$ cells, and then $CD11b+CD3^-$ cells from these. (*L* and *M*) Analysis of $CD45^+CD11b^+CD3^-$ myeloid cells in the aortic arch and the blood of these mice, showing total cells per arch or milliliter of blood. *P* values from Mann–Whitney *U* test (*C*, *E*, *J*, *L*, *M*), and ANOVA with Tukey's post hoc multiple comparison test (*F*, *H*). $^{**}P < 0.01$, $^{***}P < 0.001$, $^{****}P < 0.0001$.

ligation (18). This is an expected result, as typical in vitro culture conditions expose ECs to platelet and immune releasate in serum, and a lack of flow that removes quiescence signals normally delivered under laminar flow. Indeed, cultured EC in vitro are primed for the expression of Icam1 and Vcam1 in response to TNF-α or Il1β stimulation (5). Expression of Ptbp1 is elevated in vitro, as it is in vivo in ECs activated by exposure of LDF. Notably, the expression of Ptbp1 in vivo is not altered by flow alone, as it did not change under LDF conditions when platelets were removed. Thus, our model is that platelets are recruited to ECs exposed to LDF in vivo, where they interact with the endothelium through an unknown mechanism to induce EC priming, mediated in part by an increase in Ptbp1 expression. Our data put Ptbp1 at the intersection between platelet recruitment to the endothelium in regions of LDF, and subsequent enhanced expression of leukocyte adhesion receptors (Icam1, Vcam1, E- and P-selectin) and cytokines (Ccl2, Ccl5), leading to increased local recruitment of myeloid cells in the context of systemic TNF-α or Il1β.

Our model is consistent with the observation that not all ECs in LDF regions of aorta exhibit Vcam1 expression upon systemic LPS stimulation (4). We propose that the differential response among cells may be due to local recruitment of platelets and activation of the priming response we describe here, through increased expression of Ptbp1. Consistent with this idea, Ptbp1 expression is elevated in a subset of arterial ECs in acute and chronic exposure to LDF. Also consistent with this idea, platelets are critical for the recruitment of myeloid cells to

regions of the vasculature exposed to LDF, and also for the development of atherosclerotic plaque (14–17). Notably, the development of vascular "hotspots" of leukocyte extravasation is also dependent on platelets (36). While some of these effects are due to mechanisms previously described, such as deposition of CCL5 on the EC surface by activated platelets, and the tethering of myeloid cells to the endothelium by P-selectin expression on platelet intermediates (17), we propose that induction of Ptbp1 in the endothelium is an important consequence of platelet recruitment and contributes to the progression of vascular inflammation and plaque development. In our analysis of single-cell data, we noticed two Ptbp1-high populations: one shorter-lived, coinciding with markers of cell proliferation (Myc and Vegf signaling and ribosomal transcript production), and a longer-lived but much smaller cluster (~7% of ECs) with enriched TNF-α and hemostasis signaling. It is tempting to speculate that the long-term Ptbp1/TNF-α signaling high cells may represent the "hotspots" of leukocyte extravasation into plaque, a process which so far has lacked clear endothelial markers.

Ptbp1 and the NF-κB Signaling Pathway. Ptbp1 is widely expressed, and has been shown to regulate splicing responses and differentiation in a wide range of tissues, including neurons, cardiomyocytes, and leukocytes. While to our knowledge this work unique in showing a direct effect on the RelA/p65 nuclear translocation and NF-κB transcriptional activity, prior reports suggest that Ptbp1 effects on inflammatory responses are not limited to the endothelium. Ptbp1 was also identified in an RNA interference (RNAi) screen to identify regulators of the senescence-associated secretory phenotype (SASP) in cancer cells, indicated by expression of IL-6 and IL-8 (37). NF-κB signaling activation is critical in the induction of the SASP response, and small-interfering RNA (siRNA) to NF-κB subunit RELA suppressed the response as well. Interestingly, knockdown of Ptbp1 had little effect on the growth of cells in this screen, as we also observed in the endothelium. However, in contrast to our results in ECs, knockdown of Ptbp1 in cancer cells did not interfere with TNF-mediated induction of an NF-κB reporter (37).

The specific mediators of the effect of Ptbp1 on the NF-κB signaling pathway are not yet clear, but alterations in RNA splicing are a likely cause. RNA-binding proteins can have diverse cellular functions, including RNA transport, stability, and translation, but given the predominantly nuclear localization of the splice factor in these cells, altered nuclear splicing functions is the most likely possibility. Consistent with this idea, there is a substantial overlap between RNA splicing events regulated in vivo by the loss of platelets and those regulated in vitro by the loss of Ptbp1. The Ptbp1-suppressed alternative exon in Ripk1 we find here had been identified in screen for regulators of necroptosis in fibroblasts (26). In the Callow et al. study, they found that loss of Ptbp1 limited necroptosis, and postulated that it could be due in part to the inclusion of this premature stop codon and loss of Ripk1 protein. Although the Callow et al. study did not assess effects on NF-κB signaling, Ripk1 deficiency does not affect NF-κB activity in all cell types (38). Interestingly, it does in ECs, where knockdown of Ripk1 reduced induction of Icam1, E-selectin, and Il1B in vitro (39). In fact, ASO suppression of Ripk1 in mice limited lesion formation and necrotic core in Apoe-null mice, although the broad targeting of both endothelium and other immune and parenchymal cells limited the analysis of endothelial specific contributions (39). Given the many other changes in splicing of core and regulatory components of the NF-κB signaling pathway, it is unlikely that effects on Ripk1 are the only mediator of endothelial priming. Other notable examples include: an altered 3′UTR in Ikbkg (Nemo, a core NF-κB signaling pathway component); a skipped exon in Pdlim7 (an ubiquitin ligase of p65 which limits NF-κB signaling) (27), which adds five amino acids to a disordered region of the protein; and several genes linked to autoimmune or inflammatory diseases in human genetic association studies, such as STAT3 (3′UTR splicing; Crohn's disease, multiple sclerosis, and psoriasis) (40), FNBP1 (Cassette exon in coding region; Crohn's disease, multiple sclerosis, psoriasis, type I diabetes) (41), and MAGI1 (alternate acceptor site in coding region; Crohn's disease, psoriasis and Type-1 diabetes) (42). As the consequences of altered spicing in these transcripts is difficult to predict, future modulation of these splice isoforms will be required to understand their relative contributions.

In conclusion, we report that Ptbp1—with increased expression in regions of the vasculature exposed to LDF—is required for RelA/p65 nuclear localization and NF-κB activation upon stimulation. As loss of Ptbp1 reverts alternative splicing patterns in cultured and activated ECs toward a quiescent endothelium, and blunts the subsequent response to cytokine stimulations by TNF-α and Il1β, we propose that Ptbp1 is a critical component of EC priming by platelets. We predict that this Ptbp1 function will be conserved across different vascular beds and inflammatory responses. As Ptbp1 levels were correlated with NF-κB target genes and plaque size in human arteries, further investigation of the platelet-dependent mechanism leading to increased expression and activity of Ptbp1 and the consequences of Ptbp1-mediated splicing changes in the NF-κB signaling pathway is warranted. Importantly, interruption of this node in endothelial-platelet cross-talk suppresses EC activation and immune cell recruitment downstream of platelet responses, suggesting an approach to suppress plaque enhancing platelet functions without directly affecting platelets and critical clotting functions.

Materials and Methods

CRISPR-KO Screening. Five CRISPR-KO guide sequences were designed to each of 57 splice factor targets using described rules (Azimuth 2.0) (43), and cloned in LentiCRISPR_v2 (Addgene 52961). Lentivirus was prepared and added to recipient murine aortic endothelial cells (mAECs) at an MOI<0.3. An aliquot of cells was taken 3-4 days post infection, then from cells with highest and lowest expression of Icam1/Vcam1 or eGFP reporter of NFkB 24 hours after cytokine stimulation (30 ng/mL TNFα). Lentiviral insertions in genomic DNA were amplified by nested PCR and separated on an agarose gel for targeted sequencing. Resulting fastq files were analyzed using Mageck-0.5.6 software for guide enrichment in high-end and low-end responses.

Mice. For the endothelial deletion of Ptbp1, *Cdh5(PAC)-CreERT2* and *Ptbp1$^{lox/lox}$* mice were used, which have been previously described (33, 34). They were intercrossed to create the Ptbp1 EC-KO mice [*Cdh5(PAC)-CreERT2; Ptbp1$^{lox/lox}$*] and littermate controls (*Ptbp1$^{lox/lox}$*) used here. Mice were used between 2 and 7 mo of age in paired groups of males and females. Tamoxifen (Sigma) was delivered intraperitoneally, dissolved at 10 mg/mL in sunflower oil; 1 mg was given in each of three doses. Some mice received 100 μl intraperitoneal injections of 1 × 1011 viral particles of AAV8-encoding mutant PCSK9 (pAAV/D377Y-mPCSK9) produced at the Gene Transfer Vector Core (Grousbeck Gene Therapy Center, Harvard Medical School). Mice were then placed on the Clinton/Cybulsky high-fat rodent diet (HFD) with regular casein and 1.25% added cholesterol (D12108C; Research Diets).

All mice were housed and handled in accordance with protocols approved by the University of Connecticut Health Center for Comparative Medicine.

Analysis of Gene Expression and Splicing. RNA was isolated using an RNAeasy kit (RNAeasy, Qiagen 74104) with on column DNase treatment. For RNA-sequencing, samples were prepared for library prepraration using TruSeq RNA Library Prep Kit v2 (Illumina).

All samples were pooled into one sequencing pool, equally normalized, and run as one sample pool across the Illumina NovaSeq. Target read depth was achieved per sample with paired end 150-bp reads.

Paired-end FASTQ files were processed using Whippet (Julia 0.6.4 and Whippet v0.11) using default settings, after generating an index from GRCm38.primary_assembly.genome.fa.gz (https://www.ncbi.nlm.nih.gov/assembly/GCF_000001635.20/) and gencode.vM23.annotation.gtf.gz (https://www.gencodegenes.org/mouse/release_M23.html, Gencode, M23). Psi files and read support were used to select only splicing events with read coverage >5 across all replicates. TpM files were used to examine expression level. ggSashimi was used to plot alternative splicing events identified by Whippet analysis.

Statistical Analysis. Statistical analysis was generally performed in GraphPad Prism, with the exception of single-cell analysis (performed in Scanpy, as described in the previous section and figure legends) and GTEx analysis (performed in R using corr function). For paired samples, a Student's *t* test was performed when samples exhibited equal variance, and Mann–Whitney *U* test when variances were unequal. For comparisons among multiple samples, ANOVA with post hoc Tukey's test is used when variances are equal, and Kruskal–Wallis with post hoc Dunn's test when they are not. For analysis with multiple axis of variance (e.g., time and treatments, for cytokine responses) two-way ANOVA with post hoc Tukey's was used.

Data Availability. Processed sequencing data are available in Datasets S1–S7. Raw sequencing have been deposited in the Gene Expression Omnibus (GEO) database, https://www.ncbi.nlm.nih.gov/geo (accession no. GSE206851, https://www.ncbi.nlm.nih.gov/geo/query/acc.cgi?acc=GSE206851) (44). All other study data are included in the main text and supporting information. Previously published data were used for this work (RNA-sequencing data from refs. 18 and 22 were used, Murphy et. al., GEO accession no. GSE101826 https://www.ncbi.nlm.nih.gov/geo/query/acc.cgi?acc=GSE101826, accessed March 1, 2021 and Andueza et. al., NCBI BioProject accession no. PRJNA646233 https://www.ncbi.nlm.nih.gov/bioproject accessed Dec. 1, 2021).

ACKNOWLEDGMENTS. We thank Xenia Bradley, who worked with J.A.H. in the summer of 2017 to test conditions for the CRISPR screen that was eventually performed; Bo Reese, in the Center for Genome Innovation at UConn, for aiding in the adaptation of the CRISPR screen sequencing protocols from published work, and for being a valuable consult in RNA-sequencing studies performed here; Nathan LeClair and Olga Anczukow for sharing their plasmid minigene construct as a basis for cloning the Ripk1 minigene; and Christopher Bonin and Geneva Hargis in the Science Writing and Illustration group at UConn Health, for editing and help with our graphical abstract. In the course of this work, we received valuable input from the ImmunoCardiovascular Group at UConn Health, particularly Dr. Beiyan Zhou (University of Connecticut) and Alison Kohan (University of Pittsburgh). This work was supported by UConn Health startup funds from the School of Medicine and Department of Cell Biology, Center for Vascular Biology and Calhoun Cardiology Center, American Heart Association Innovative Project Award 19IPLOI34770151 (to P.A.M.); NIH National Heart, Lung, and Blood Institute Grants K99/R00-HL125727 and R01-HL150362 (to P.A.M); and American Heart Association Predoctoral awards (to J.A.H. and S.-A.E.N.).

Author affiliations: [a]Center for Vascular Biology, UConn Health, University of Connecticut, Farmington, CT 06030; [b]Department of Immunology, UConn Health, University of Connecticut, Farmington, CT 06030; and [c]Institute of Medical Science, University of Tokyo, 113-8654 Tokyo, Japan

1. K. Ley, C. Laudanna, M. I. Cybulsky, S. Nourshargh, Getting to the site of inflammation: The leukocyte adhesion cascade updated. *Nat. Rev. Immunol.* **7**, 678–689 (2007).
2. M. A. Gimbrone Jr., G. García-Cardeña, Endothelial cell dysfunction and the pathobiology of atherosclerosis. *Circ. Res.* **118**, 620–636 (2016).
3. R. Gareus *et al.*, Endothelial cell-specific NF-kappaB inhibition protects mice from atherosclerosis. *Cell Metab.* **8**, 372–383 (2008).
4. L. Hajra *et al.*, The NF-kappa B signal transduction pathway in aortic endothelial cells is primed for activation in regions predisposed to atherosclerotic lesion formation. *Proc. Natl. Acad. Sci. U.S.A.* **97**, 9052–9057 (2000).
5. G. Dai *et al.*, Distinct endothelial phenotypes evoked by arterial waveforms derived from atherosclerosis-susceptible and -resistant regions of human vasculature. *Proc. Natl. Acad. Sci. U.S.A.* **101**, 14871–14876 (2004).
6. N. Baeyens, C. Bandyopadhyay, B. G. Coon, S. Yun, M. A. Schwartz, Endothelial fluid shear stress sensing in vascular health and disease. *J. Clin. Invest.* **126**, 821–828 (2016).
7. Z. Al-Yafeai *et al.*, Endothelial FN (fibronectin) deposition by α5β1 integrins drives atherogenic inflammation. *Arterioscler. Thromb. Vasc. Biol.* **38**, 2601–2614 (2018).
8. A. W. Orr *et al.*, The subendothelial extracellular matrix modulates NF-kappaB activation by flow: A potential role in atherosclerosis. *J. Cell Biol.* **169**, 191–202 (2005).
9. R. E. Feaver, B. D. Gelfand, C. Wang, M. A. Schwartz, B. R. Blackman, Atheroprone hemodynamics regulate fibronectin deposition to create positive feedback that sustains endothelial inflammation. *Circ. Res.* **106**, 1703–1711 (2010).
10. P. A. Murphy *et al.*, Alternative splicing of FN (fibronectin) regulates the composition of the arterial wall under low flow. *Arterioscler. Thromb. Vasc. Biol.* **41**, e18–e32 (2021).
11. V. Henn *et al.*, CD40 ligand on activated platelets triggers an inflammatory reaction of endothelial cells. *Nature* **391**, 591–594 (1998).
12. M. S. Garshick *et al.*, Activated platelets induce endothelial cell inflammatory response in psoriasis via COX-1. *Arterioscler. Thromb. Vasc. Biol.* **40**, 1340–1351 (2020).
13. S. Nhek *et al.*, Activated platelets induce endothelial cell activation via an interleukin-1β pathway in systemic lupus erythematosus. *Arterioscler. Thromb. Vasc. Biol.* **37**, 707–716 (2017).
14. S. Massberg *et al.*, A critical role of platelet adhesion in the initiation of atherosclerotic lesion formation. *J. Exp. Med.* **196**, 887–896 (2002).
15. S. Massberg *et al.*, Platelet adhesion via glycoprotein IIb integrin is critical for atheroprogression and focal cerebral ischemia: An in vivo study in mice lacking glycoprotein IIb. *Circulation* **112**, 1180–1188 (2005).
16. P. C. Burger, D. D. Wagner, Platelet P-selectin facilitates atherosclerotic lesion development. *Blood* **101**, 2661–2666 (2003).
17. Y. Huo *et al.*, Circulating activated platelets exacerbate atherosclerosis in mice deficient in apolipoprotein E. *Nat. Med.* **9**, 61–67 (2003).
18. P. A. Murphy *et al.*, Alternative RNA splicing in the endothelium mediated in part by Rbfox2 regulates the arterial response to low flow. *eLife* **7**, e29494 (2018).
19. N. K. Leclair *et al.*, Poison exon splicing regulates a coordinated network of SR protein expression during differentiation and tumorigenesis. *Mol. Cell* **80**, 648–665.e9 (2020).
20. L. Zhang *et al.*, Novel pathological role of hnRNPA1 (heterogeneous nuclear ribonucleoprotein A1) in vascular smooth muscle cell function and neointima hyperplasia. *Arterioscler. Thromb. Vasc. Biol.* **37**, 2182–2194 (2017).
21. E. Engelbrecht *et al.*, Sphingosine 1-phosphate-regulated transcriptomes in heterogenous arterial and lymphatic endothelium of the aorta. *eLife* **9**, e52690 (2020).
22. A. Andueza *et al.*, Endothelial reprogramming by disturbed flow revealed by single-cell RNA and chromatin accessibility study. *Cell Rep.* **33**, 108491 (2020).
23. A. S. Kalluri *et al.*, Single-cell analysis of the normal mouse aorta reveals functionally distinct endothelial cell populations. *Circulation* **140**, 147–163 (2019).
24. M. A. C. Depuydt *et al.*, Microanatomy of the human atherosclerotic plaque by single-cell transcriptomics. *Circ. Res.* **127**, 1437–1455 (2020).
25. A. A. Wilson *et al.*, Lentiviral delivery of RNAi for in vivo lineage-specific modulation of gene expression in mouse lung macrophages. *Mol. Ther.* **21**, 825–833 (2013).
26. M. G. Callow *et al.*, CRISPR whole-genome screening identifies new necroptosis regulators and RIPK1 alternative splicing. *Cell Death Dis.* **9**, 261 (2018).
27. A. Jodo, A. Shibazaki, A. Onuma, T. Kaisho, T. Tanaka, PDLIM7 synergizes with PDLIM2 and p62/Sqstm1 to inhibit inflammatory signaling by promoting degradation of the p65 subunit of NF-κB. *Front. Immunol.* **11**, 1559 (2020).
28. E. Monzón-Casanova *et al.*, Polypyrimidine tract-binding proteins are essential for B cell development. *eLife* **9**, e53557 (2020).
29. E. Monzón-Casanova *et al.*, The RNA-binding protein PTBP1 is necessary for B cell selection in germinal centers. *Nat. Immunol.* **19**, 267–278 (2018).
30. C. J. David, M. Chen, M. Assanah, P. Canoll, J. L. Manley, HnRNP proteins controlled by c-Myc deregulate pyruvate kinase mRNA splicing in cancer. *Nature* **463**, 364–368 (2010).
31. X. Han *et al.*, Using Mendelian randomization to evaluate the causal relationship between serum C-reactive protein levels and age-related macular degeneration. *Eur. J. Epidemiol.* **35**, 139–146 (2020).
32. P. M. Ridker *et al.*; Pravastatin or Atorvastatin Evaluation and Infection Therapy-Thrombolysis in Myocardial Infarction 22 (PROVE IT-TIMI 22) Investigators, C-reactive protein levels and outcomes after statin therapy. *N. Engl. J. Med.* **352**, 20–28 (2005).
33. I. Sörensen, R. H. Adams, A. Gossler, DLL1-mediated Notch activation regulates endothelial identity in mouse fetal arteries. *Blood* **113**, 5680–5688 (2009).
34. T. Shibasaki *et al.*, PTB deficiency causes the loss of adherens junctions in the dorsal telencephalon and leads to lethal hydrocephalus. *Cereb. Cortex* **23**, 1824–1835 (2013).
35. M. Roche-Molina *et al.*, Induction of sustained hypercholesterolemia by single adeno-associated virus-mediated gene transfer of mutant hPCSK9. *Arterioscler. Thromb. Vasc. Biol.* **35**, 50–59 (2015).
36. G. Zuchtriegel *et al.*, Platelets guide leukocytes to their sites of extravasation. *PLoS Biol.* **14**, e1002459 (2016).
37. A. Georgilis *et al.*, PTBP1-mediated alternative splicing regulates the inflammatory secretome and the pro-tumorigenic effects of senescent cells. *Cancer Cell* **34**, 85–102.e9 (2018).
38. W. W.-L. Wong *et al.*, RIPK1 is not essential for TNFR1-induced activation of NF-kappaB. *Cell Death Differ.* **17**, 482–487 (2010).
39. D. Karunakaran *et al.*, *RIPK1* expression associates with inflammation in early atherosclerosis in humans and can be therapeutically silenced to reduce NF-κB activation and atherogenesis in mice. *Circulation* **143**, 163–177 (2021).
40. S. E. Flanagan *et al.*, Activating germline mutations in STAT3 cause early-onset multi-organ autoimmune disease. *Nat. Genet.* **46**, 812–814 (2014).
41. R. Nakamura *et al.*, A multi-ethnic meta-analysis identifies novel genes, including ACSL5, associated with amyotrophic lateral sclerosis. *Commun. Biol.* **3**, 526 (2020).
42. A. Julià *et al.*, A deletion at ADAMTS9-MAGI1 locus is associated with psoriatic arthritis risk. *Ann. Rheum. Dis.* **74**, 1875–1881 (2015).
43. J. G. Doench *et al.*, Optimized sgRNA design to maximize activity and minimize off-target effects of CRISPR-Cas9. *Nat. Biotechnol.* **34**, 184–191 (2016).
44. J. A. Hensel *et al.*, Splice Factor Polypyrimidine tract-binding protein 1 (Ptbp1) Primes Endothelial Inflammation in Atherogenic Disturbed Flow Conditions. GEO. https://www.ncbi.nlm.nih.gov/geo/query/acc.cgi?acc=GSE206851. Deposited 24 June 2022.